Current Biology 22, 1693–1698, September 25, 2012 ©2012 Elsevier Ltd All rights reserved http://dx.doi.org/10.1016/j.cub.2012.07.002

Report

Neuroanatomical Assessment of Biological Maturity

Timothy T. Brown,[1,2,*] Joshua M. Kuperman,[1,3] Yoonho Chung,[1,4] Matthew Erhart,[1,3] Connor McCabe,[4] Donald J. Hagler, Jr.,[1,3] Vijay K. Venkatraman,[1,3] Natacha Akshoomoff,[4,5] David G. Amaral,[7] Cinnamon S. Bloss,[8] B.J. Casey,[9] Linda Chang,[10] Thomas M. Ernst,[10] Jean A. Frazier,[11] Jeffrey R. Gruen,[12] Walter E. Kaufmann,[13,17] Tal Kenet,[14] David N. Kennedy,[11] Sarah S. Murray,[8] Elizabeth R. Sowell,[15,16] Terry L. Jernigan,[3,4,5,6] and Anders M. Dale[1,2,3,5,6]

[1]Multimodal Imaging Laboratory, University of California, San Diego, School of Medicine, La Jolla, CA 92037, USA
[2]Department of Neurosciences
[3]Department of Radiology
[4]Center for Human Development
[5]Department of Psychiatry
[6]Department of Cognitive Science
University of California, San Diego, La Jolla, CA 92093, USA
[7]Department of Psychiatry and Behavioral Sciences, University of California, Davis, Davis, CA 95817, USA
[8]Scripps Genomic Medicine, Scripps Translational Science Institute and Scripps Health, La Jolla, CA 92037, USA
[9]Sackler Institute for Developmental Psychobiology, Weil Cornell Medical College, New York, NY 10065, USA
[10]Department of Medicine, University of Hawaii and Queen's Medical Center, Honolulu, HI 96813, USA
[11]Department of Psychiatry, University of Massachusetts Medical School, Boston, MA 01605, USA
[12]Departments of Pediatrics and Genetics, Yale University School of Medicine, New Haven, CT 06520, USA
[13]Kennedy Krieger Institute, Johns Hopkins University School of Medicine, Baltimore, MD 21205, USA
[14]Department of Neurology and Athinoula A. Martinos Center for Biomedical Imaging, Massachusetts General Hospital, Charlestown, MA 02129, USA
[15]Department of Pediatrics, University of Southern California, Los Angeles, Los Angeles, CA 90027, USA
[16]Children's Hospital, Los Angeles, CA 90027, USA

Summary

Structural MRI allows unparalleled in vivo study of the anatomy of the developing human brain. For more than two decades [1], MRI research has revealed many new aspects of this multifaceted maturation process, significantly augmenting scientific knowledge gathered from postmortem studies. Postnatal brain development is notably protracted and involves considerable changes in cerebral cortical [2–4], subcortical [5], and cerebellar [6, 7] structures, as well as significant architectural changes in white matter fiber tracts [8–11] (see [12]). Although much work has described isolated features of neuroanatomical development, it remains a critical challenge to characterize the multidimensional nature of brain anatomy, capturing different phases of development among individuals. Capitalizing on key advances in multisite, multimodal MRI, and using cross-validated nonlinear modeling, we demonstrate that developmental brain phase can be assessed with much greater precision than has been possible using other biological measures, accounting for more than 92% of the variance in age. Further, our composite metric of morphology, diffusivity, and signal intensity shows that the average difference in phase among children of the same age is only about 1 year, revealing for the first time a latent phenotype in the human brain for which maturation timing is tightly controlled.

Results

In order to measure and model individual differences in biological brain maturity, we employed several new advances that provide the ability to integrate data from across different imaging modalities and from across different sites and scanners. We used a standardized, multimodal structural MRI protocol implemented at nine different institutions on 12 different scanners made by three different manufacturers. Data were collected in a deliberately diverse sample of 885 typically developing individuals between 3 and 20 years old (see Table S1 and Supplemental Information available online). The human research protections programs and institutional review boards at the universities participating in this study approved all experimental and consenting procedures. Our acquisition protocol included new techniques for crossmodal nonlinear image registration [13], scanner-specific distortion corrections [14], and adjustments for other site and scanner effects through the application of multisite correction offsets. Fully automated postprocessing algorithms, including atlas-based white matter tractography [15], were then used to produce a brain-wide set of anatomical biomarkers. Two hundred thirty one structural brain features known or suspected to change over the ages studied here were measured in every individual. This collection of variables was derived from T1-, T2-, and diffusion-weighted imaging and included quantitative measures of brain morphology, signal intensity, and water diffusivity within different tissue types, reflecting anatomical structural organization. Specifically, we measured cortical thickness and area, volumes of segmented subcortical structures, normalized signal intensities, and measures of diffusion magnitude and directionality within cerebral, cerebellar, and white matter fiber tract regions of interest (see Supplemental Information for a complete list of measures).

Individual Brain Measures

Individual neuroanatomical measures varied greatly in the degree to which they changed with age, in the ages at which they matured, and in their individual differences variability, showing increases, decreases, or nonmonotonic changes (Figure 1). For example, mean cortical thickness decreased almost linearly with age and matured relatively late, continuing to decline through age 20. In contrast, total cortical area increased until the age of 12.3 years and then declined

[17]Present address: Department of Neurology, Boston Children's Hospital and Harvard Medical School, Boston, MA 02115, USA
*Correspondence: ttbrown@ucsd.edu

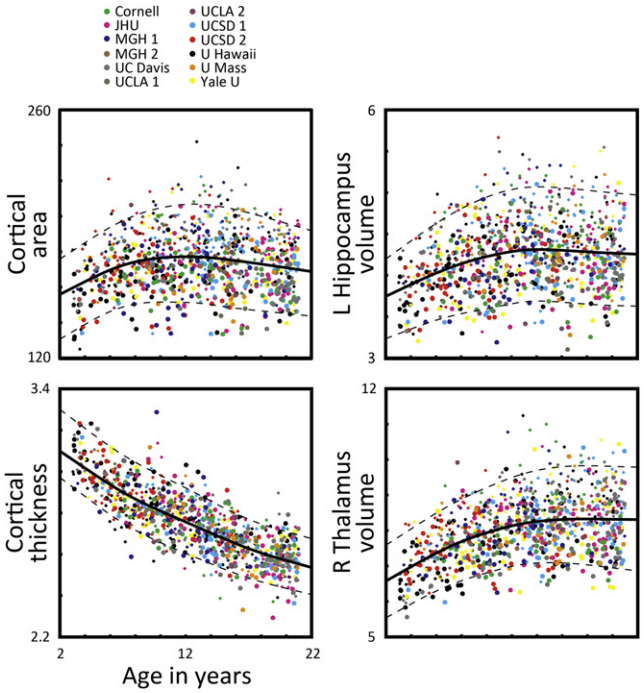

Figure 1. Individual Measures Derived from the T1-Weighted Imaging Protocol

Example measures derived from the segmentation of the T1-weighted volume are plotted for 885 subjects as a function of age: total cortical area in square millimeters by thousands, mean cortical thickness in millimeters, volume of the left hippocampus in cubic millimeters by thousands, and volume of the right thalamus in cubic millimeters by thousands. Colors correspond to different sites and scanners. Symbol size represents subject sex (larger = female, smaller = male). A spline-fit curve (solid line) with 5% and 95% prediction intervals (dashed lines) are also shown.

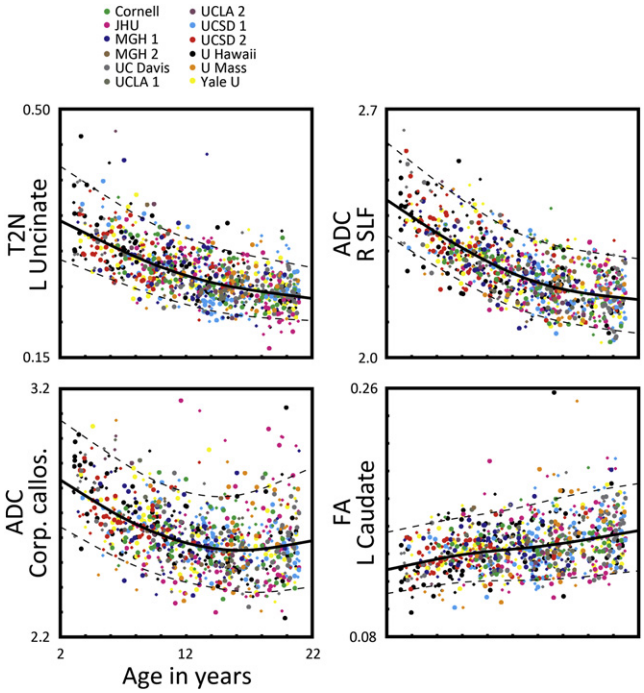

Figure 2. Individual Measures Derived from the T2- and Diffusion-Weighted Imaging Protocols

Example measures derived from the T2- and diffusion-weighted protocols are plotted for 885 subjects as a function of age: T2-normalized (T2N) signal intensity of left uncinate fibers; apparent diffusion coefficient (ADC) of the corpus callosum; ADC of the right superior longitudinal fasciculus (SLF); and fractional anisotropy (FA) of the left caudate nucleus. Colors correspond to different sites and scanners. Symbol size represents subject sex (larger = female, smaller = male). A spline-fit curve (solid line) with 5% and 95% prediction intervals (dashed lines) are also shown.

somewhat but showed comparatively high and constant variability by age. Hippocampal volume increased until the age of 14.2 before slightly decreasing. Volume of the thalamus showed smaller individual differences variability at younger ages and, though peaking at age 17.8, essentially continued in a plateau to age 20.

Cerebral, cerebellar, and white matter tract diffusivity and signal intensity measures also varied greatly in their developmental profiles (Figure 2). For example, apparent diffusion coefficient (ADC), a measure of the overall magnitude of water diffusion, decreased steadily to age 20 in right superior longitudinal fasciculus (SLF). This fiber tract connects posterior brain regions to anterior brain regions. ADC in corpus callosum fibers, on the other hand, declined, reached a nadir at age 16.3, and then slightly increased, showing a different developmental trajectory for fibers connecting the two cerebral hemispheres. T2-normalized signal intensity, associated with myelin content and white matter integrity [16, 17], decreased in the left uncinate fasciculus and showed somewhat decreasing variability with age. This tract connects portions of the limbic system to the frontal lobes. Fractional anisotropy (FA), reflecting the directionality of water movement within tissue, showed age-related increases in the left caudate nucleus, where there was a slight acceleration at about age 14.

Composite Developmental Phase Metric

Our standardized, fully integrated multimodal acquisition and analysis approach allowed us to combine all of the individual biomarkers into a brain-wide, multidimensional model of human structural brain development. In order to capitalize on each measure's idiosyncratic contribution to capturing biological changes across age and to test the degree to which a combination of these measures assesses the overall phase of individual brain development, we employed a cross-validated multivariate fitting procedure. Using a multivariate distance measure and leave-one-out cross-validation, we determined the age that provides the best fit for each subject by comparing measures for that subject to smooth, nonlinear age trajectories (of the mean and covariance) derived from all other individuals (see Supplemental Information for details). This method was chosen in order to empirically calculate the degree of multicollinearity among the predictor variables, to remove redundant variance through rotation, orthogonalization, and normalization, and to guard stringently against overfitting. Including 231 variables derived from multiple imaging modalities, the resulting neuroanatomical model accounted for over 92% of the individual differences variability in developmental brain phase as defined by chronological age (Rho = 0.961, R-squared = 0.923; Figure 3). This model had a mean prediction error across all ages of just 1.03 years and was most accurate in predicting brain maturity at the youngest ages we studied, where annualized neuroanatomical changes are greatest in most measures.

In order to compare the separate contributions of the different imaging modalities—and thus types of biological change—to brain maturity, we then divided the multimodal

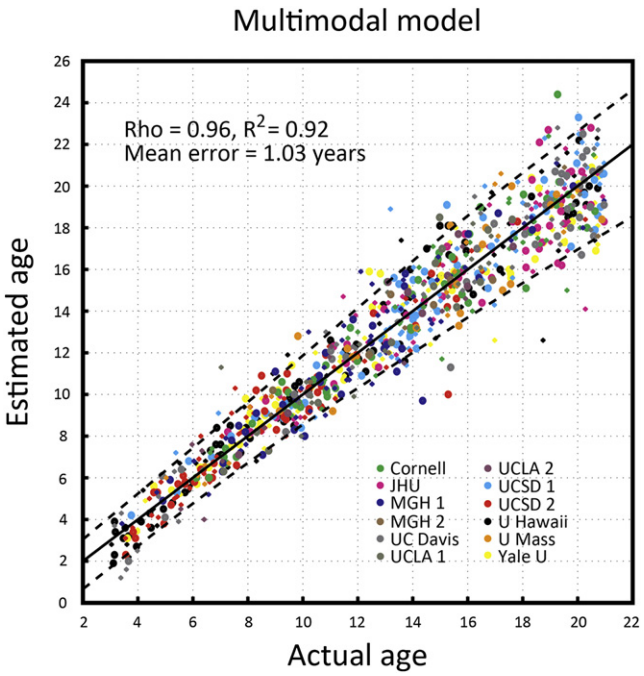

Figure 3. Multimodal Quantitative Anatomical Prediction of Age

For 885 individuals, estimated brain age is plotted as a function of actual chronological age. Colors correspond to different sites and scanners. Symbol size represents subject sex (larger = female, smaller = male). A spline-fit curve (solid line) with 5% and 95% prediction intervals (dashed lines) is also shown.

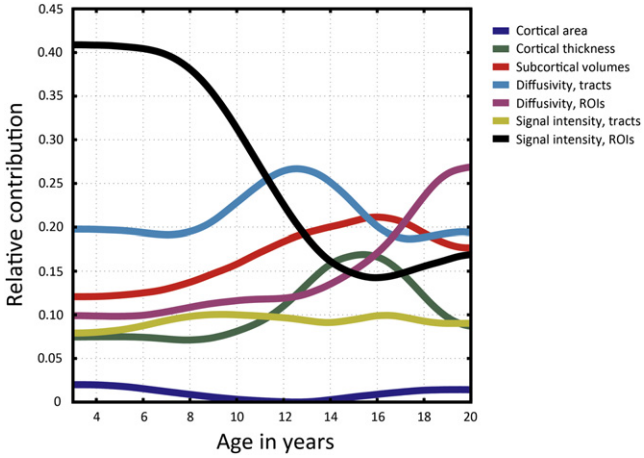

Figure 4. Age-Varying Contributions of Different Imaging Measures to the Prediction of Age

The relative contributions of separate morphological, diffusivity, and signal intensity measures within different brain structures are plotted as a function of age. Colors correspond to measure and structure type (dark blue, T1 cortical area; green, T1 cortical thickness; red, T1 subcortical volumes; light blue, diffusion (FA/ADC) within white matter tracts; dark pink, diffusion (FA/ADC) within subcortical ROIs; gold, T2 signal intensity within white matter tracts; black, T2 signal intensity within subcortical ROIs). Contributions are computed as units of the proportion of total explained variance.

model into three mutually exclusive subsets of measures derived from either the T1-, diffusion-, or T2-weighted scans. The T1 subset model, comprised of 45 measures of cortical area and thickness and subcortical structure volumes, accounted for 83% of the individual differences variability in age (Rho = 0.910, R-squared = 0.828) and showed an average prediction error of 1.71 years across all ages we studied. The diffusion model, made up of the 124 measures of diffusivity (FA, ADC) in subcortical structures and white matter tracts, captured 81% of the variance in age (Rho = 0.898, R-squared = 0.806) and also had a mean prediction error of 1.71 years. The T2 model, comprised of 62 signal intensity measures within subcortical regions of interest (ROIs) and white matter tracts, accounted for 83% of the variance across the full age range (Rho = 0.910, R-squared = 0.828, mean error = 1.60 years; see figures in Supplemental Information).

Despite similar predictive power for the full age range, the age-varying contributions of different imaging modalities to the composite model varied widely across measure type and within different neuroanatomical structures (Figure 4). At the youngest ages, from about 3 to 11 years old, measures of T2 signal intensity within subcortical ROIs were by far the strongest predictors of developmental phase, declining in importance through the early teens. Diffusion measures within white matter fiber tracts, in comparison, were consistently strong predictors across the age range, becoming the highest contributor during the middle ages of about 12 to 15. T1-derived morphological measures varied, with cortical thickness and subcortical volumes contributing more than cortical area, which was consistently the weakest predictor over age. Interestingly, diffusivity measures within subcortical ROIs increased sharply at about age 14 and were the strongest maturational predictors at the oldest ages, from about 17 to 20 years old.

Discussion

In developing a composite neuroanatomical metric of biological maturity, we sought to address several fundamental questions about the multidimensional nature of human brain development—questions that could not easily be answered using conventional methods looking at individual brain characteristics in isolation. First, can a combination of noninvasive brain biomarkers accurately assess the dynamically changing phases of brain development from early childhood into young adulthood, and to what degree of precision? Inherently, developmentalists have been interested in the timing aspects of unfolding biological changes, so chronological age has been a key anchor by which many have sought to characterize biological maturity. Conventional medical approaches for assessing biological maturity in childhood and adolescence have focused on the study of somatic growth (e.g., height, weight, body build) [18], dental age [19], skeletal age [20], and hormonal and secondary sexual characteristics [21]. Although clinically informative for placing individuals with regard to age-referenced norms, the high interindividual variability and subjectivity of these measures make them of limited use in predicting age or of conveying much about a child's complex biological development. Other recent biological approaches to age prediction have used DNA methylation [22], which explained 73% of the variability in age from 18 to 70 years old, and resting state fMRI data [23], which accounted for 55% of the variance between the ages of 7 and 30. Because functional and structural imaging methods would be expected to capture different types of individual differences variability, it might be useful to combine neuroanatomical biomarkers with dynamic physiological measures, such as from functional

MRI, electroencephalography (EEG), or magnetoencephalography (MEG). The degree to which these imaging and recording techniques can be combined to model brain development, or to predict cognitive and behavioral functioning, remain open empirical questions.

Second, which types of neuroanatomical measures are most powerful for capturing developmental changes across these ages? Separate models of morphology, diffusivity, and signal intensity accounted for similarly high amounts of variance across the full age range at 83%, 81%, and 83% respectively. It is notable that even without any information about the size (i.e., area, thickness, volume) of growing brain structures, maturational phase across a relatively broad developmental span is still captured about equally well using only knowledge about the changing tissue properties. Currently, there is widespread interest in the development of brain connectivity and the belief that protracted white matter changes underpin some of the latest-maturing human cognitive abilities [24, 25]. Our results show that composite diffusivity and signal intensity measures provide a useful index of maturation derived directly from measures of the brain's connections themselves (i.e., white matter fiber tracts). Future studies will need to determine whether and how these measures relate specifically to the brain's changing profile of connectedness.

On a related note, do the relative contributions of these different biological measures to explaining individual differences change with age and, if so, how? A direct comparison of the age-varying contributions of the measures, broken down further by different types of neuroanatomical structures, shows a complex, dynamic cascade of changes with different features dominating at different points along the developmental trajectory. It is interesting that measures of T2 signal intensity within subcortical ROIs, not within major cerebral white matter tracts, have the highest phase prediction power up until the age of about 11. Inspection of the individual biomarkers reveals that signal intensity specifically within bilateral pallidum accounts for a large proportion of this overall effect, consistent with a known developmental iron accumulation phenomenon within the basal ganglia [26]. In comparison, diffusion magnitude and directionality within fiber tracts were strong predictors more consistently across the entire age range. Although these measures are commonly collected in child imaging studies and would likely be expected to be useful in predicting maturity, it is informative to see their collective contribution compared directly with other measures and modalities across this age span. As with any biomarker, we surmised that a T1-derived morphological measure that has small individual differences dispersion relative to its annualized change, such as mean cortical thickness, would be better at distinguishing developmental phase than a measure with relatively large variability and little relative change, such as total cortical area. Comparing the individual scatterplot for area with its age-varying contribution, one can see that the measure's usefulness to prediction becomes zero at exactly the age it asymptotes. Although researchers commonly look at FA and ADC (or mean diffusivity) within major fiber tracts, fewer have published diffusion data within subcortical cerebral and cerebellar gray and white matter. For this reason, it is particularly interesting that the predictive strength of diffusivity measures within subcortical ROIs increased sharply at about age 14 and was the strongest developmental predictor from about 17 to 20 years old. The specific contributions of individual measures within this set of variables should be further characterized because of their apparently important role in development specifically at older ages.

A critical developmental question and a point of great speculation among scientists, educators, and parents is this: To what extent do children of the same age differ among each other in their degree of biological maturity? This issue is of fundamental importance to our understanding of human development and is especially relevant to the development of the brain because it underpins all of cognition and behavior. In explaining more than 92% of the variance in age, the multimodal neuroanatomical approach shows an as yet unrivaled ability to capture different phases of biological maturity and, as a result, reveals for the first time a latent brain phenotype for which the maturational timing is tightly controlled. Across the first two decades of postnatal development, there is on average only about 1 year (1.03 years) of difference in this composite metric of neuroanatomical maturity among individuals of the same age, and this difference gradually increases from preschool age into young adulthood. Among 3-year-old children, there is only about 8 months (0.66 years) difference on average in this developmental phase metric. At age 12, this difference is just under 1 year (0.95 years), and at age 20 it is only about 1 year and 5 months (1.42 years). It is interesting and somewhat surprising that the multimodal metric captures so much of the individual differences variance and across such a wide developmental range. This demonstrates that, despite marked variability among children across a wide variety of isolated brain measures, there are aspects of brain development for which the multidimensional biological phase is remarkably controlled, and its timing is more closely tied to chronological age than was previously known. It should be made clear that these results do not refute the fact that same-aged children exhibit great variability in their psychological functioning, such as in their cognitive, behavioral, social, and academic abilities. Brain scans, though informative about anatomical and physiological states, cannot be used to make inferences about an individual's psychological maturity. Rather, these results speak only to the degree to which typically developing children differ among each other in their fundamental structural brain properties. Nevertheless, this finding is compelling because it addresses a longstanding scientific question by establishing the existence of a highly homochronous neuroanatomical phenotype.

Looking further at the developmental metric, although the composite differences are generally small at a given age, there are some individuals for whom maturational brain phase is notably over- or underpredicted for their chronological age. For example, the multimodal scatter plot shows a 15-and-a-half year-old girl with a predicted brain age of 10, as well as a 7-year-old boy with a maturity metric of about 11.3 years. Are these children developmentally delayed or precocious in any other way that we can identify? Because we recruited an intentionally diverse group of subjects (see Supplemental Information), our sample likely includes a relatively wide range of individual differences in brain structure, with many intrinsic and extrinsic contributing factors. In exploring and developing this approach further, we will carefully examine all of the individuals who are atypical according to this developmental phase metric, looking for systematic cognitive, behavioral, medical history, and genetic differences. MRI research to date has begun to reveal the structural brain correlates of many common neurodevelopmental disorders, including autism [27], attention disorders [28, 29], and language [30]

and reading [31] disorders. Perhaps further development of techniques to quantify the complex multidimensional nature of typical brain maturation can also help to improve the early identification of individuals with abnormal developmental trajectories. Our findings suggest that a multimodal neuroanatomical imaging assessment may hold promise for making an objective, quantitative contribution to our clinical evaluations of brain development.

One limitation of the multidimensional approach is that the models can be difficult to understand in terms of the original measures if they become too complex. For example, an unwieldy number of predictor variables or the use of data reduction techniques such as factor analysis may make results less easily interpretable. For this reason, we used regularization without any abstracted factor transformation such as independent components analysis or machine learning. It can also be helpful to test the separate elements of the model in several ways, as we have done, so as to clarify the relative contributions of different types of measures to the overall biological maturity metric.

In conclusion, our study shows that noninvasive, imaging-based biomarkers can be used to assess different phases of human brain maturity, producing a highly precise biological metric of an individual's age. Measures of brain morphology, diffusivity, and signal intensity show varying contributions to the prediction of developmental phase at different ages, reflecting a dynamic cascade of biological changes within different tissue types. Perhaps most interestingly, our findings precisely quantify the multidimensional variability that exists in human neuroanatomical growth, revealing for the first time a latent brain phenotype that is tightly linked to chronological age. According to this composite measure, over the first two decades of postnatal development, individuals of the same age show an average phase difference of only about 1 year. This collection of multimodal, multisite imaging advances now makes it possible for researchers across institutions to establish large-scale, shared databases that can be explored with unprecedented power in order to address critical scientific and clinical questions about human brain health and disease.

Supplemental Information

Supplemental Information includes four figures, two tables, and Supplemental Experimental Procedures and can be found with this article online at http://dx.doi.org/10.1016/j.cub.2012.07.002.

Acknowledgments

The authors gratefully thank the children, adolescents, adults, and parents who participated in the research. Data used in preparation of this study were obtained from the Pediatric Imaging, Neurocognition, and Genetics Study (PING) database. As such, the investigators within PING contributed to the design and implementation of PING and/or provided data but did not necessarily participate in the analysis or writing of this report. A complete listing of PING investigators can be found at http://ping.chd.ucsd.edu. Data collection and sharing for this project was funded by PING (National Institutes of Health grant RC2DA029475), which is funded by the National Institute on Drug Abuse and the Eunice Kennedy Shriver National Institute of Child Health and Human Development. PING data are disseminated by the PING Coordinating Center at the Center for Human Development, University of California, San Diego. A.M.D. is a founder of and holds equity interest in CorTechs Labs, La Jolla, CA, and serves on its scientific advisory board. The terms of this arrangement have been reviewed and approved by the University of California, San Diego in accordance with its conflict of interest policies.

Received: April 16, 2012
Revised: June 20, 2012
Accepted: July 2, 2012
Published online: August 16, 2012

References

1. Jernigan, T.L., Trauner, D.A., Hesselink, J.R., and Tallal, P.A. (1991). Maturation of human cerebrum observed in vivo during adolescence. Brain *114*, 2037–2049.
2. Giedd, J.N., Blumenthal, J., Jeffries, N.O., Castellanos, F.X., Liu, H., Zijdenbos, A., Paus, T., Evans, A.C., and Rapoport, J.L. (1999). Brain development during childhood and adolescence: a longitudinal MRI study. Nat. Neurosci. *2*, 861–863.
3. Shaw, P., Kabani, N.J., Lerch, J.P., Eckstrand, K., Lenroot, R., Gogtay, N., Greenstein, D., Clasen, L., Evans, A., Rapoport, J.L., et al. (2008). Neurodevelopmental trajectories of the human cerebral cortex. J. Neurosci. *28*, 3586–3594.
4. Sowell, E.R., Peterson, B.S., Thompson, P.M., Welcome, S.E., Henkenius, A.L., and Toga, A.W. (2003). Mapping cortical change across the human life span. Nat. Neurosci. *6*, 309–315.
5. Ostby, Y., Tamnes, C.K., Fjell, A.M., Westlye, L.T., Due-Tønnessen, P., and Walhovd, K.B. (2009). Heterogeneity in subcortical brain development: A structural magnetic resonance imaging study of brain maturation from 8 to 30 years. J. Neurosci. *29*, 11772–11782.
6. Caviness, V.S., Jr., Kennedy, D.N., Richelme, C., Rademacher, J., and Filipek, P.A. (1996). The human brain age 7-11 years: a volumetric analysis based on magnetic resonance images. Cereb. Cortex *6*, 726–736.
7. Tiemeier, H., Lenroot, R.K., Greenstein, D.K., Tran, L., Pierson, R., and Giedd, J.N. (2010). Cerebellum development during childhood and adolescence: a longitudinal morphometric MRI study. Neuroimage *49*, 63–70.
8. Lebel, C., and Beaulieu, C. (2011). Longitudinal development of human brain wiring continues from childhood into adulthood. J. Neurosci. *31*, 10937–10947.
9. Paus, T., Zijdenbos, A., Worsley, K., Collins, D.L., Blumenthal, J., Giedd, J.N., Rapoport, J.L., and Evans, A.C. (1999). Structural maturation of neural pathways in children and adolescents: in vivo study. Science *283*, 1908–1911.
10. Westlye, L.T., Walhovd, K.B., Dale, A.M., Bjørnerud, A., Due-Tønnessen, P., Engvig, A., Grydeland, H., Tamnes, C.K., Ostby, Y., and Fjell, A.M. (2010). Life-span changes of the human brain white matter: diffusion tensor imaging (DTI) and volumetry. Cereb. Cortex *20*, 2055–2068.
11. Mukherjee, P., Miller, J.H., Shimony, J.S., Conturo, T.E., Lee, B.C., Almli, C.R., and McKinstry, R.C. (2001). Normal brain maturation during childhood: developmental trends characterized with diffusion-tensor MR imaging. Radiology *221*, 349–358.
12. Giedd, J.N., and Rapoport, J.L. (2010). Structural MRI of pediatric brain development: what have we learned and where are we going? Neuron *67*, 728–734.
13. Holland, D., and Dale, A.M.; Alzheimer's Disease Neuroimaging Initiative. (2011). Nonlinear registration of longitudinal images and measurement of change in regions of interest. Med. Image Anal. *15*, 489–497.
14. Holland, D., Kuperman, J.M., and Dale, A.M. (2010). Efficient correction of inhomogeneous static magnetic field-induced distortion in Echo Planar Imaging. Neuroimage *50*, 175–183.
15. Hagler, D.J., Jr., Ahmadi, M.E., Kuperman, J., Holland, D., McDonald, C.R., Halgren, E., and Dale, A.M. (2009). Automated white-matter tractography using a probabilistic diffusion tensor atlas: Application to temporal lobe epilepsy. Hum. Brain Mapp. *30*, 1535–1547.
16. Glasser, M.F., and Van Essen, D.C. (2011). Mapping human cortical areas in vivo based on myelin content as revealed by T1- and T2-weighted MRI. J. Neurosci. *31*, 11597–11616.
17. Hagmann, C.F., De Vita, E., Bainbridge, A., Gunny, R., Kapetanakis, A.B., Chong, W.K., Cady, E.B., Gadian, D.G., and Robertson, N.J. (2009). T2 at MR imaging is an objective quantitative measure of cerebral white matter signal intensity abnormality in preterm infants at term-equivalent age. Radiology *252*, 209–217.
18. Wutscherk, H. (1974). Die Bestimmung des biologischen Alters. Theor. Und Praxis der Korperkultur *23*, 169–170.
19. Demirjian, A., Goldstein, H., and Tanner, J.M. (1973). A new system of dental age assessment. Hum. Biol. *45*, 211–227.

20. Tanner, J.M., Whitehouse, R.H., and Healy, M.J.R. (1962). A New System for Estimating Skeletal Maturity from the Hand and Wrist, with Standards Derived from a Study of 2,600 Healthy British Children. Parts I and II (Paris: Centre International de l'Enfance).
21. Tanner, J.M. (1963). The Regulation of Human Growth. Child Dev. *34*, 817–847.
22. Bocklandt, S., Lin, W., Sehl, M.E., Sánchez, F.J., Sinsheimer, J.S., Horvath, S., and Vilain, E. (2011). Epigenetic predictor of age. PLoS ONE *6*, e14821.
23. Dosenbach, N.U., Nardos, B., Cohen, A.L., Fair, D.A., Power, J.D., Church, J.A., Nelson, S.M., Wig, G.S., Vogel, A.C., Lessov-Schlaggar, C.N., et al. (2010). Prediction of individual brain maturity using fMRI. Science *329*, 1358–1361.
24. Nagy, Z., Westerberg, H., and Klingberg, T. (2004). Maturation of white matter is associated with the development of cognitive functions during childhood. J. Cogn. Neurosci. *16*, 1227–1233.
25. Paus, T. (2005). Mapping brain maturation and cognitive development during adolescence. Trends Cogn. Sci. *9*, 60–68.
26. Aoki, S., Okada, Y., Nishimura, K., Barkovich, A.J., Kjos, B.O., Brasch, R.C., and Norman, D. (1989). Normal deposition of brain iron in childhood and adolescence: MR imaging at 1.5 T. Radiology *172*, 381–385.
27. Courchesne, E., Campbell, K., and Solso, S. (2011). Brain growth across the life span in autism: age-specific changes in anatomical pathology. Brain Res. *1380*, 138–145.
28. Sowell, E.R., Thompson, P.M., Welcome, S.E., Henkenius, A.L., Toga, A.W., and Peterson, B.S. (2003). Cortical abnormalities in children and adolescents with attention-deficit hyperactivity disorder. Lancet *362*, 1699–1707.
29. Mackie, S., Shaw, P., Lenroot, R., Pierson, R., Greenstein, D.K., Nugent, T.F., 3rd, Sharp, W.S., Giedd, J.N., and Rapoport, J.L. (2007). Cerebellar development and clinical outcome in attention deficit hyperactivity disorder. Am. J. Psychiatry *164*, 647–655.
30. Watkins, K.E., Vargha-Khadem, F., Ashburner, J., Passingham, R.E., Connelly, A., Friston, K.J., Frackowiak, R.S., Mishkin, M., and Gadian, D.G. (2002). MRI analysis of an inherited speech and language disorder: structural brain abnormalities. Brain *125*, 465–478.
31. Eckert, M. (2004). Neuroanatomical markers for dyslexia: a review of dyslexia structural imaging studies. Neuroscientist *10*, 362–371.